2023-01-01

Resuspension of microplastics and microrubbers in a semi-arid urban environment (Shiraz, Iran)

Khodabakhshloo, N

http://hdl.handle.net/10026.1/20499

10.1016/j.envpol.2022.120575
Environmental Pollution
Elsevier BV

Resuspension of microplastics and microrubbers in a semi-arid urban environment (Shiraz, Iran)

Nafiseh Khodabakhshloo [a], Sajjad Abbasi [a]*, Andrew Turner [c]

[a] Department of Earth Sciences, College of Science, Shiraz University, Shiraz 71454, Iran

[c] School of Geography, Earth and Environmental Sciences, University of Plymouth, PL4 8AA, UK

https://doi.org/10.1016/j.envpol.2022.120575

Accepted 31 October 2022

Abstract

Although airborne urban particulates are a concern for air quality and human health, little information exists on the levels and characteristics of microplastics (MPs) and microrubbers (MRs) in this setting. In the present study, MPs and MRs are quantified and characterised in road dusts and accumulations captured passively (and up to elevations of about 1.8 m above road level) in the steps of utility poles at 18 locations throughout the city of Shiraz, southwest Iran. Dust accumulation rates were greatest at road level (median = 45 g m^{-2} $month^{-1}$) and declined with elevation (median = 2.0 g m^{-2} $month^{-1}$ at 177 cm). The concentrations (per g of dust) and accumulation of MPs and MRs were more variable between locations but accumulation declined with elevation for both particle types and MR concentration (up to ~27,000 MR g^{-1}) was always greater than corresponding MP concentration (up to ~3300 MP g^{-1}). Increasing elevation was also accompanied by an increasing proportion of fine ($\leq$ 100 μm) and fibrous particles, and in particular for MPs. Fractionation in the quantities and characteristics with elevation above road level are attributed to the extent of resuspension of MPs and MRs from the road surface by wind and passing traffic, with aerodynamic considerations predicting the greatest and most widespread resuspension of fibrous MPs. The fractionation of MPs and MRs with elevation above road level also result in different exposures for adults and children.

Keywords: dusts; street; aerodynamic; exposure; accumulation; fibres

1. Introduction

Road dust is a heterogeneous reservoir of particulate matter arising from various sources, including abrasion of the road surface and mechanical vehicle components, exhaust emissions from traffic, and deposition of regional airborne geogenic and biogenic particles (Thorpe and Harrison, 2008). In turn, settled road dust represents a secondary source of airborne particulate matter when fine particles are resuspended back into the local atmosphere through wind and passing vehicles, and especially under dry conditions (Rogge et al., 1993; Panko et al., 2013; Fussell et al., 2022).

In urban environments, resuspension of road dust is an increasing concern for air quality and human health. With vehicle exhaust emissions being progressively regulated, it has been suggested that resuspension is at least as significant to the population of particles having aerodynamic diameters less than 10 μm (PM_{10}) and for respiratory and cardiovascular health as exhaust sources (Kuenan et al., 2014; Weinbruch et al., 2014; Thouron et al., 2018). As a consequence, there have been attempts to empirically model road dust emissions and exposures, but this is often hampered by a lack of knowledge of the resuspension process itself, and the complex effects of different vehicle categories, driving behaviours, road surfaces and climates on emissions (Ventrakam, 2000; Escrig et al., 2011). As an alternative, emissions have also been estimated more directly through mass balance calculations and the measurement of source materials or tracers collected by passive sampling devices deployed at different elevations above the street surface (Wagner and Leith, 2001; Amato et al., 2012).

Particles from tyre wear, largely made up of natural and synthetic rubbers, have been recognized as an important contributor to road dust in the urban setting (Alvez et al., 2020; Moskovchenko et al., 2022). However, relatively little quantitative information exists on their abundance, through direct microscopic imagery or via some chemical marker of tire tread, for example, or their resuspension from the road surface (Abbasi et al., 2019; Panko et al., 2019; Youn et al., 2021). Moreover, and despite the ubiquity of microplastics (MPs, and comprising synthetic, petroleum-based polymers) and the extensive literature addressing their importance in the atmosphere (Dris et al., 2016; Liu et al., 2019; Brahney et al., 2020; Abbasi et al., 2022), even less information exists on their occurrence in road dusts (Abbasi et al., 2019; Järlskog et al., 2020; O'Brien et al., 2021). Significantly, and as far as we are aware, there has been no consideration of MPs in relation to their resuspension from a road surface as a secondary, urban source.

In the present study, we consider both MPs and microrubbers (MRs, and dominated by tire wear particulates) in road dusts and material sampled passively at different elevations above street level in Shiraz, a large, semi-arid city in southwest Iran. MPs and MRs are identified, discriminated and characterised by established techniques and differences in particle characteristics as a function of elevation are used to infer information about their sources, resuspension from the road surface and potential for human exposure in the urban setting.

2. Materials and methods

2.1. Study area and sample collection

Sampling was undertaken within the Shiraz metropolitan district of southwest Iran (population ~ 2 M). Urbanized Shiraz covers an area of about 240 km^2 that lies on the plain of a seasonal river with underlying sedimentary rocks at an elevation of about 1600 m above sea level. The climate is moderate semi-arid, with an annual average rainfall and temperature of 335 mm and 18 ^oC, respectively, and a prevailing wind from the north to north-west (average annual wind speed is 2.35 m s^{-1}).

Air pollution in Shiraz results from primitive forms of heating, traffic, agriculture and various manufacturing, processing and refining industries (mainly related to cement and oil production and energy generation). Air quality in the city has been declining over recent years because of growth in population and urbanization and an increasing incidence of dust storms (Abbasi et al., 2022).

Sampling was conducted during the dry season in 2021 at 17 sites within different municipal sectors of Shiraz (urban, residential, industrial-commercial, recreational) and at a control location to the northwest and upwind of the city and at an altitude of about 1900 m above sea level (Ghalat) (Figure 1). At each site, the three lower steps (or 485 cm^2 cavity floors) of a 12-m concrete utility pole (at elevations of 23 cm, 101 cm and 177 cm above the pavement) and a semicircular 1570 cm^2 area of the (asphalt) road surface adjacent to the kerb were cleaned using distilled water and with the aid of a pre-cleaned horsehair wooden brush in May (Figure 1). During October, and a after a passive sampling period of about 150 days, the sites were re-visited and material that had accumulated over the five-month period was transferred onto individual sheets of aluminium foil with the aid of the brush and a stainless steel dustpan. Any visible debris, including leaves, cigarette butts and pieces of paving stone, asphalt, concrete and brick, were manually removed before the contents were carefully wrapped and sealed.

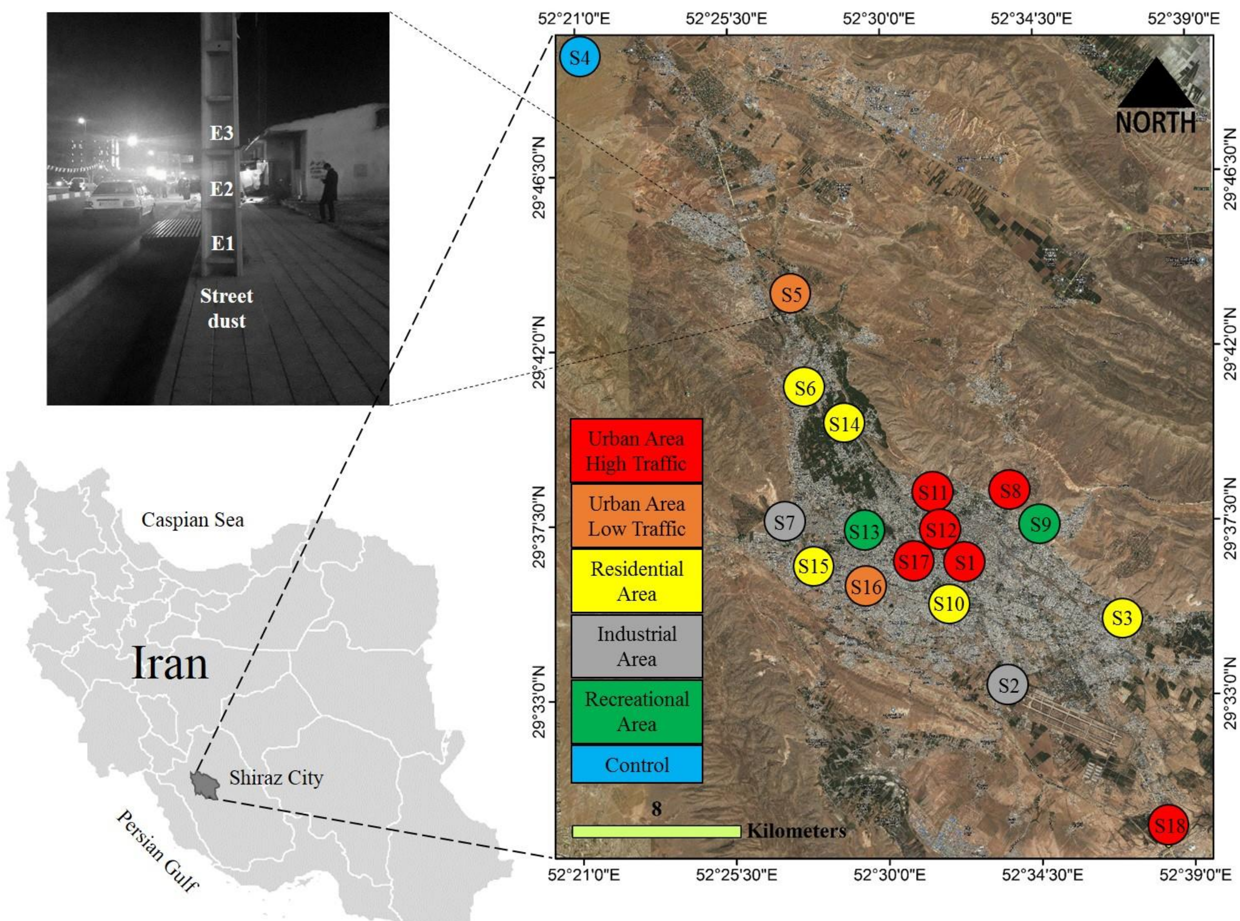

Fig 1. Sampling locations and their municipal categorisation in Shiraz, southwest Iran. The photograph shows a concrete utility pole and the lower three steps (E1, E2 and E3) used for passive sampling

2.2. MP and MR isolation

For the isolation, identification and characterisation of MPs and MRs in the dusts, we followed previously published methods and quality assurance protocols with some modifications (Abbasi et al., 2017, Abbasi et al., 2019). Briefly, samples (*n* = 72) were sieved through a 5-mm metal mesh, with fractionated material weighed on a Libror AEL-40SM balance (Shimadzu, Kyoto). Fractionated material (between about 10 and 100 g of street dust and 0.1 to 5 g of utility pole dust), plus four controls (in the absence of weighted material), was mixed with 100 to 200 mL of 35% filtered H_2O_2 (Arman Sina, Tehran) for several days (and until bubble formation ceased) in a series of covered, glass 50 mL beakers. Remaining H_2O_2 was removed by evaporation in a sand bath at 50^{o}C before 50 mL of filtered, saturated $ZnCl_2$ solution (Arman Sina, Tehran) was added to each beaker. The contents were agitated for 5 min at 350 rpm and then allowed to settle for 90 min. Supernatants were centrifuged for 3 min at 4000 rpm before being vacuum-filtered through S&S filter papers (blue band, grade 589/3, 2 μm pore size) and washed with distilled water. The process of settling, centrifuging, and filtering was repeated three times through the same filter and dried filters were stored in individual, sealed petri dishes.

2.3. MP and MR analysis

Whole filters or precisely measured fractions thereof were observed under a stereo digital microscope (Sairan DSM3000) at 200 x magnification with the aid of ImageJ software. MPs were identified by their hardness, gloss, uniform thickness and reaction to a hot needle (Hidalgo-Ruz et al., 2012), while MRs were identified by their distinctively non-glossy, black appearance, high elasticity and propensity to reversibly deform (Abbasi et al., 2019). MPs and MRs were classified according to shape as: fiber, film, fragment or spherule; size in terms of length or primary diameter, L, as: fine ($L \leq 100$ μm), intermediate ($100 < L \leq 1000$ μm) or coarse ($L > 1000$ μm); and, for MP fibres, thickness or diameter, d, as: thin (≤ 10 μm), medium ($10 < d \leq 20$ μm) and thick ($d > 30$ μm).

The polymeric composition of a selection of MPs from different locations and of different sizes and shapes ($n = 30$) was determined using a micro-Raman spectrometer (LabRAM HR, Horiba, Japan) with a laser of 785 nm, a Raman shift of 400–1800 cm^{-1} and acquisition times between 20 and 30 s.

3. Results

3.1. Accumulation of dust

The net accumulation rates of material (dust) at each location and elevation in Shiraz are shown in Table 1. Here, rates were calculated at E0 (road level) and E1, E2 and E3 (23 cm, 101 cm and 177 cm above the pavement, respectively, and within cavities of the utility poles) from the mass of material accumulated over a specific area for a period of about 150 days.

Inter-location variations in deposition rates are evident at all levels; for example, deposition at road level ranges from about 16 g m^{-2} $month^{-1}$ in an urban setting subject to high traffic flow (S1) to 120 g m^{-2} $month^{-1}$ in a residential area (S10). Variations likely reflect the complex interplay of a number of factors relating to the proximity and significance of local dust sources, land use, microclimate and effects of any buildings on such, topography, surface roughness and road and utility pole orientation relative to wind direction. By contrast, variations in accumulation rates as a function of elevation are more consistent amongst different locations and there were no differences that could be attributable to utility pole orientation. Thus, in all but two cases, rates were greatest at street level (E0); at ten locations, rates declined progressively with increasing elevation, and at all locations, the lowest rates were observed at the greatest elevation (ranging from < 0.1 to 6.6 g m^{-2} $month^{-1}$).

Table 1: Net accumulation rates of material at road level and at different elevations for each location.

	accumulation, g m^{-2} $month^{-1}$			
location	E0	E1	E2	E3
S1	16.1	1.9	3.6	0.2
S2	77.6	1.9	2.3	1.1
S3	48.7	8.8	3.4	0.4
S4	52.6	7.3	1.6	1.1
S5	31.4	7.8	12.2	5.1
S6	34.5	7.1	5.0	3.1
S7	43.7	6.2	3.0	3.0
S8	51.2	6.8	12.3	1.4
S9	45.3	23.0	12.9	6.1
S10	118.1	3.4	1.4	1.1
S11	36.2	19.3	9.0	2.6
S12	21.0	21.5	10.3	5.6
S13	63.6	5.7	7.1	5.3
S14	58.5	10.5	13.5	6.6
S15	66.1	3.6	0.2	<0.1
S16	44.7	2.1	1.5	1.0
S17	32.3	34.2	17.9	1.1
S18	23.5	3.1	0.1	<0.1
median	45.0	6.9	4.3	2.0

Table 2: Abundance and net accumulation rates (mo = month) of MPs and MRs at road level and the different elevations sampled at each location. Note, insufficient material was obtained for E3 at S15 and S18 and that median values exclude the corresponding control measurements (at S4).

	E0				E1				E2				E3			
location	MP g^{-1}	MP m^{-2} mo^{-1}	MR g^{-1}	MR m^{-2} mo^{-1}	MP g^{-1}	MP m^{-2} mo^{-1}	MR g^{-1}	MR m^{-2} mo^{-1}	MP g^{-1}	MP m^{-2} mo^{-1}	MR g^{-1}	MR m^{-2} mo^{-1}	MP g^{-1}	MP m^{-2} mo^{-1}	MR g^{-1}	MR m^{-2} mo^{-1}
S1	120.6	1936.3	770.3	12366.9	690.0	1323.7	8432.9	16177.3	122.8	445.4	729.1	2643.3	708.0	132.0	1150.4	214.4
S2	119.2	9248.4	728.3	56501.9	1719.3	3233.0	5375.0	10107.2	1770.2	4041.2	850.8	1942.3	154.1	173.2	231.1	259.8
S3	40.5	1972.0	165.0	8040.8	479.0	4210.3	1206.1	10602.1	915.0	3092.8	790.5	2672.2	143.9	57.7	20.6	8.2
S4	0.7	35.7	1.5	79.0	1.1	8.2	6.8	49.5	12.7	20.6	12.7	20.6	0	0	0	0
S5	3.2	99.4	397.2	12458.6	14.7	115.5	743.5	5822.7	4.7	57.7	18.2	222.7	4.0	20.6	10.5	53.6
S6	70.2	2421.7	808.9	27913.4	378.2	2696.9	1509.4	10762.9	952.6	4771.1	7421.4	37171.1	155.9	482.5	56.0	173.2
S7	38.5	1682.8	68.1	2975.8	67.7	420.6	531.4	3303.1	47.1	140.2	94.3	280.4	11.0	33.0	16.4	49.5
S8	82.8	4238.2	799.2	40922.3	172.8	1167.0	3850.0	25995.9	106.4	1307.2	191.6	2354.6	59.9	86.6	376.7	544.3
S9	124.4	5631.8	978.8	44305.7	44.2	1014.4	199.0	4569.1	133.6	1723.7	185.3	2391.8	36.6	222.7	41.3	251.5
S10	24.2	2857.3	192.9	22777.1	105.7	358.8	2164.2	7348.5	722.0	1018.6	926.6	1307.2	40.6	45.4	77.6	86.6
S11	135.3	4894.3	931.1	33671.3	64.2	1241.2	2688.0	51991.8	193.9	1736.1	402.1	3600.0	49.9	132.0	656.8	1736.1
S12	181.0	3805.1	836.8	17589.8	96.2	2066.0	1659.5	35645.4	300.3	3096.9	633.5	6532.0	178.6	993.8	16.3	90.7
S13	17.3	1101.9	292.8	18608.9	81.1	461.9	1739.6	9901.0	56.6	404.1	587.8	4193.8	23.2	123.7	66.4	354.6
S14	34.6	2021.7	181.0	10588.5	155.7	1628.9	607.5	6354.6	20.5	276.3	105.5	1422.7	23.8	156.7	5.0	33.0
S15	24.2	1597.5	200.6	13253.5	621.3	2235.1	3020.4	10866.0	3338.3	828.9	7573.5	1880.4				
S16	44.1	1969.4	315.7	14109.6	167.0	358.8	11556.6	24828.9	414.6	630.9	2945.8	4482.5	77.6	74.2	107.8	103.1
S17	80.2	2588.5	951.4	30726.1	77.2	2643.3	878.2	30070.1	50.6	903.1	50.1	894.8	429.3	461.9	161.0	173.2
S18	135.8	3188.5	670.6	15740.1	151.3	461.9	3837.6	11715.5	1645.6	214.4	27025.3	3521.6				
median*	70.2	2421.7	670.6	17589.8	151.3	1241.2	1739.6	10762.9	193.9	903.1	633.5	2391.8	59.9	132.0	66.4	173.2

3.2. Accumulation of MPs and MRs

The abundance (per g of sample) and net accumulation rates (per m^2 per month) of MPs and MRs are shown at each elevation for all locations in Table 2. The values of all measures except for MP abundance at E2 were lowest at the control site, with maximum values at each elevation at least two orders of magnitude greater than corresponding controls and encountered across all municipal categories of Shiraz shown in Figure 1 except for urban areas with low traffic. Median values (excluding control data) are shown as measures of central tendency after it was established that most data sets were non-normally distributed.

According to a series of Wilcoxon signed rank tests performed in Minitab *v*19, MP abundance was significantly greater ($p < 0.05$) at E1 and E2 than at E0 and E3, and MP accumulation was significantly greater at E0 than the remaining elevations. Wilcoxon tests also established significantly greater medians in MR abundance and accumulation rates than in corresponding MP abundance and accumulation rates at E0, E1 and E2, but no significant differences between particle types were observed in either measure at E3.

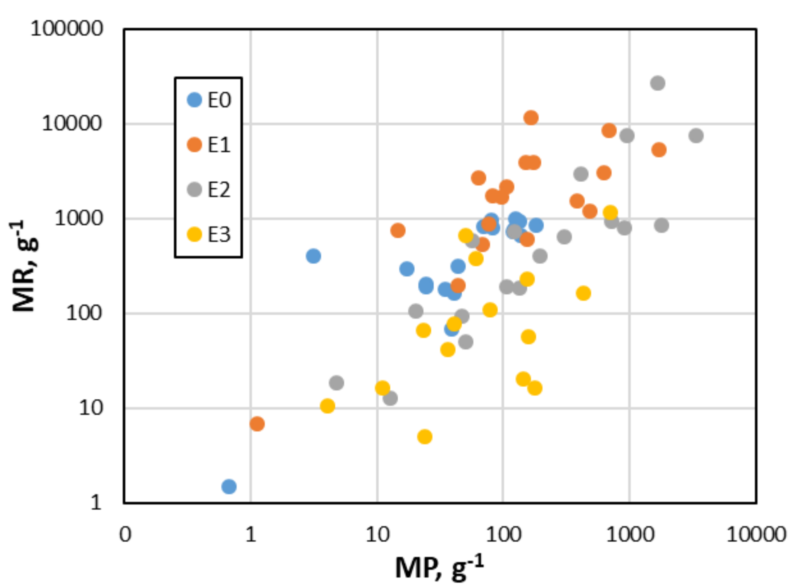

Figure 2: Abundance of MRs versus abundance of MPs and grouped by elevation.

Figure 2 is a scatter plot of the abundance of MRs against the abundance of MPs. Overall, and for each elevation, data were significantly related ($p < 0.05$) according to Pearson's moment correlation, with equivalent analyses of MRs and MPs on an accumulation basis resulting in significant, albeit weaker correlations. Median ratios of MR to MP abundance (or measures of the slopes of the relationships in Figure 2) were about 15 at E0 and E1, but decreased to about 4 and 2.3 at E2 and E3, respectively.

3.3. Characteristics of MPs and MRs

The distribution of MPs and MRs by shape and size at each location and elevation is illustrated in Figure 3. Specifically, Figures 3a and 3b show the percentages of fibres in MPs and MRs, respectively, with remaining particles being films and fragments (MR spherules were only observed at S8, E1), while Figures 3c and 3d show the percentages of fine ($L \leq 100$ μm) particles in MPs and MRs, respectively, with the majority of remaining particles being large ($L > 1000$ μm) at E0 and intermediate ($L = 100$ to 1000 μm) above road level. At all locations, there is an increase in the percentage of fibrous MPs above road level (where the range is 13 to 88%), and in many cases at one or more of E1, E2 or E3 the entire MP population is made up of fibres. The percentage of fibrous MRs is considerably lower (and never exceeds 25% overall and 5% at road level), and in most (but not all) cases, fibres are more abundant at elevation than at road level. At all locations, the percentage of fine MPs is higher at E1, E2 and E3 than at road level, and while the distribution of fine MRs is more complex, the highest percentages are usually found at E3.

Regarding MP fibre diameter, the overall distribution was: 88.8% thin, 7.9% medium, and 3.3% thick. At road level, however, there was a greater percentage of thick fibres and a smaller percentage of thin fibres compared with corresponding values at the remaining elevations, and thick fibres were completely absent at ten sites at E3.

Figure 3: Percentage of (a) fibres in MPs, (b) fibres in MRs, (c) fine MPs ($L \leq 100$ μm) and (d) fine MRs ($L \leq 100$ μm) at road level and the different elevations of each sampling location.

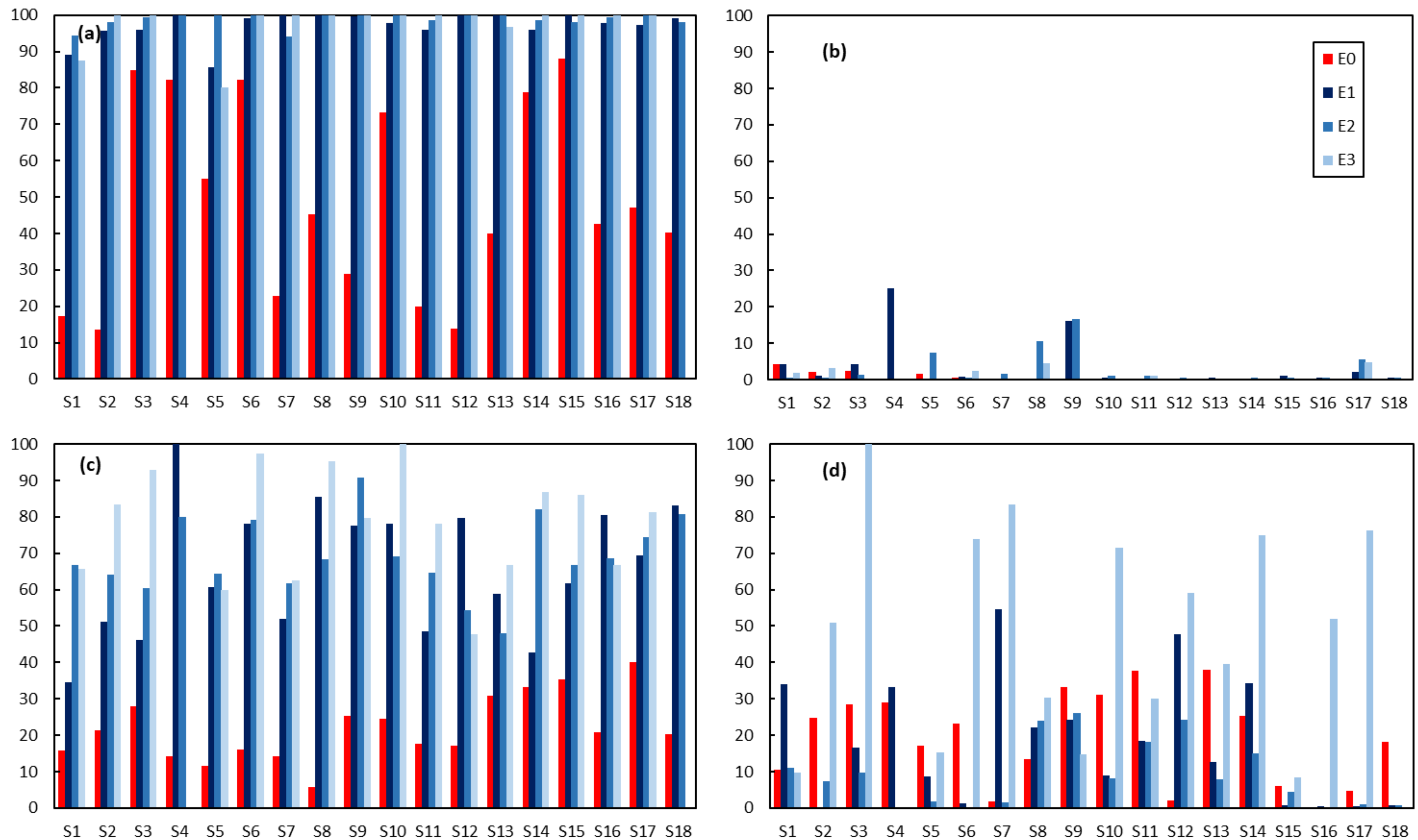

(a)
(b)
(c)
(d)
E0
E1
E2
E3
S1 S2 S3 S4 S5 S6 S7 S8 S9 S10 S11 S12 S13 S14 S15 S16 S17 S18
0 10 20 30 40 50 60 70 80 90 100

The results of the Raman analysis of selected MPs are shown in Table 3. The most commonly encountered polymers amongst the fibres analysed (*n* = 21) were polyethylene terephthalate and nylon, with polypropylene, polyvinylchloride, polyester, chlorinated polyisoprene and polyurethane also detected. Amongst the fragments analysed (*n* = 9), polyethylene was present in three cases, with polyethylene terephthalate, polypropylene, nylon and polyvinylchloride also detected.

Table 3: Polymeric composition of MPs analysed by micro-Raman spectrometry (*n* = 30).

polymer	fibres	fragments
polyethylene terephthalate	9	2
polypropylene	2	2
nylon	3	1
polyethylene	0	3
polyvinylchloride	2	1
polyester-epoxy	2	0
chlorinated polyisoprene	2	0
polyurethane	1	0

4. Discussion

The accumulation of MPs and MRs in the urban setting is likely controlled by many of the factors that are responsible for the accumulation of urban dusts more generally, including microclimate, topography, vegetation, surface roughness, the effects of buildings on airflow and proximity to direct sources (Weber et al., 2014; Mei et al., 2018; Zhao et al., 2018). Local, direct sources of MPs and MRs in the urban environment include households, offices, artificial turfs, littering, manufacturing industries, building construction and renovation, waste disposal, thermoplastic road markings, and traffic (Dris et al., 2016; Wang et al., 2020; Järlskog et al., 2020; Kitahara and Nakata, 2020; Yukioka et al., 2020), with the latter in the form of vehicle tires particularly significant for MRs (NIVA, 2020; Fussell et al., 2022). More distant, diffuse sources represent the aggregation of these and other sources (including agriculture) over a wider area (Abbasi et al., 2022). The heterogeneity in the abundance and characteristics of MPs and MRs across the locations and municipal sectors in Shiraz, therefore, reflects variations in the significance of such sources and factors, but overall accumulation is greater than at the control location where direct sources, including those associated with traffic and industry, are less important.

There is little quantitative information on MPs and MRs in road dusts and comparisons are not straightforward because of different methodologies involved in sample collection and processing, the impacts of different climates (and in particular, rainfall) on material accumulation and dispersal, and different approaches adopted to isolate, define and analyse plastics and rubbers. For instance, Patchaiyappan et al. (2021) report a mean and standard deviation of MP concentrations in < 5 mm urban dusts from Chennai of just 0.23 ± 0.09 MP g^{-1} following flotation in saturated NaCl solution (density ~ 1200 kg m^{-3}), and while Järlskog et al. (2020) report a concentration of 2.6 MPs and MRs combined per g of > 100 μm sweepsand from streets in Gothenburg after flotation in NaCl, this increased to about 10 per g when a denser solution of saturated NaI (density ~ 1850 kg m^{-3}) was employed. By comparison, when pyrolysis-gas chromatography-mass spectrometry has been used, O'Brien et al. (2021) report selected MPs (according to polymer type) in street dusts from Queensland up to 5.9 mg MP g^{-1}, while measurements of the MR content of road dusts and roadside PM10 are on the order of a few percent by weight (Panko et al., 2019; Youn et al., 2021).

More directly comparable with the results of the present study are measurements of MP and MR abundance in road dusts of other cities in Iran where a similar climate is encountered and broadly common protocols (including identification criteria and size fractionation) have been adopted and as summarized in Table 4. Thus, the range and medians of MP concentrations are of similar orders of magnitude for the large cities of Shiraz and Tehran and the smaller coastal cities of Asaluyeh and Bushehr, but MR concentrations in Shiraz are considerably higher than those reported for Asaluyeh and Bushehr where traffic intensity is relatively low.

Table 4: A summary of MP and MR concentrations in road dusts from Iran.

	MP g^{-1}			MR g^{-1}			Source
City	min	max	median	min	max	median	
Asaluyeh	3.5	515.0	14.8	2.5	88.3	7.1	Abbasi et al. (2019)
Bushehr	21.0	165.8		4.4	78.2		Abbasi et al. (2017)
Shiraz	3.2	181.0	70.2	68.1	978.8	670.6	This study
Tehran	2.9	20.2	6.1				Dehghani et al. 2017

While the quantities of MPs and MRs captured by specifically designed sampling devices (Brahney et al., 2020) or sampled after specific events (Abbasi et al., 2022) can be employed to estimate depositional fluxes from the atmosphere, net accumulation rates at the street surface are not necessarily equivalent to this measure, even in the absence of precipitation. This is because material deposited by the kerbside is subject to resuspension and redistribution through the action of wind and pedestrians, air disturbance from passing traffic, and capture and transportation by vehicle tyres (Venkatram, 2000; Adachi and Tainosho, 2004; Cai and Li, 2019; Rienda and Alves, 2021). Accumulation of MPs and MRs by passive samplers, like the more sheltered utility pole steps, may provide better estimates of depositional rates because material captured is subject to fewer interventions (Amato et al., 2012). However, the fixed orientation and indented structure of these steps also constrain their use in this respect. Nevertheless, the relative accumulation (or concentration) of MPs and MRs at different elevations may provide useful information on the transport and potential impacts of these particles in the urban setting.

At road level, net accumulation of MPs and MRs reflects the deposition and redistribution of particles emitted from traffic close to the road and derived from other local (non-traffic) sources and a more general, urban background. At elevation, general urban particulate deposition and the redistribution of traffic sources through resuspension assume greater relative significance. At different elevations (E1, E2 and E3) it would be reasonable to assume that general atmospheric deposition is the same and that any differences in the quantities and characteristics of particles arise, therefore, through the resuspension of material at street level. This results in a decrease in the amount of material (dust) with increasing elevation and a shift in the fractionation of lighter MPs and MRs on a number, shape and size basis. Specifically, the quantities of MPs and MRs per g of dust increase up to E1 (1 m) and decrease at E3 (1.77 m) while the proportions of fine and fibrous MPs and MRs are persistently (and often progressively) higher at elevation compared with road level. These observations reflect a combination of distance (elevation) from the road surface and fractionation of the particle properties that govern resuspension, including aerodynamic size and density (Thatcher and Layton, 1995; Rienda and Alvez, 2021). They also suggest that there is no significant preferential retention of fine MPs and MRs within the microstructure of the road surface (NIVA, 2020).

Overall, the shift in fractionation with elevation is greater for MRs than MPs, suggesting that the transport of MRs is more limited. Thus, according to median abundances (per g) in Table 2 (and excluding the control location), the ratio of MRs to MPs is about 10 at E0 and E1, 3.3 at E2, and 1.1 at E3. Although the density of the principal source of urban rubber (tire particles, about 840 kg m^{-3}; Li et al., 2004) is lower than that of MPs (between about 900 and 1500 kg m^{-3} for the polymers identified in Table 3), this may be increased by the incorporation of road surface materials on abrasion to 1200 to 1700 kg m^{-3} (NIVA, 2020; Jung and Choi, 2022). Moreover, the shape and size of MRs are more constraining on their transportation relative to thin, fibrous MPs, effects that can be demonstrated by comparing particle settling velocities in air for MRs and MPs of equal *L*.

Thus, according to Henn (1996), the Stokesian (or effective spherical) diameter, d_s, of a fibre of 100 μm in length and a representative, measured diameter, *d*, of 5 μm (aspect ratio, $\beta = L/d$, of 20):

$$d_s \sim (\ln 2\beta)^{1/2} d \qquad (1)$$

is about 9.6 μm (and, therefore, classified as PM_{10}). For a microplastic density, ρ_{MP}, of 1000 kg m^{-3}, d_s is also equal to an aerodynamic equivalent diameter, d_a:

$$d_a \sim (\rho_{MP} \ln 2\beta)^{1/2} d \qquad (2)$$

The settling velocity, v_s, of such a fibre is given by:

$$v_s = (\rho_{MP} - \rho_{air}) g d_s^2 / 18\eta \qquad (3)$$

where ρ_{air} is the density of air at 25°C (= 1.17 kg m^{-3}) and η is its viscosity (= 18.6 x 10^{-6} m^2 s^{-1}), and is equal to about 0.0027 m s^{-1}. For a polymer of density 1500 kg m^{-3}, v_s is about 0.004 m s^{-1} according to equation 3. By comparison, the settling velocities of fragments of MR of densities, ρ_{MR}, 840 kg m^{-3} and 1200 kg m^{-3}, and *d* = 100 μm can be modelled as quasi-spheres (the mode of distribution of circularity of tire wear particles is 0.83; Kreider et l., 2010):

$$v_s = (\rho_{MR} - \rho_{air})gd^2/18\eta \qquad (4)$$

resulting in settling velocities of about 0.25 m s^{-1} and 0.35 m s^{-1}, respectively. Despite uncertainties regarding fragment shape, a difference in v_s of two orders of magnitude between the two particle types illustrates the greater mobility and susceptibility for atmospheric transport for urban MP fibres relative to urban MR fragments.

Qualitatively, these observations and calculations are consistent with findings in the literature. For example, Pandey et al. (2022) found that while fragments dominated the MP population on the street of an Indian city, fibres dominated MPs in the atmosphere at an elevation of 7.5 m. Panko et al. (2013) showed that < 1% of PM_{10} sampled at 1.5 to 2.5 m above the ground in various urbanised districts in the US, Europe and Japan was made up of tire and road wear particles, suggesting that the majority of fine MRs remain at road level.

The direct and indirect impacts of airborne MPs and MRs on human health are unclear, and in particular at realistic levels of exposure (Abbasi et al., 2019; Fussell et al., 2022). However, they are likely to depend on factors such as size, shape, polymeric composition and the nature and availability of any additives or chemicals acquired from the environment (Amato-Lourenço et al., 2020; Vethaak and Legler, 2020). Nevertheless, in terms of exposure in the urban setting, the present study is significant in demonstrating fractionation of characteristics of MPs and MRs that are believed to be critical to respiratory health through an elevation of less than 2 m. Thus, at 1.77 m (E3), representative of the height of an adult, particles are less abundant (relative to other solids), more fibrous (at least for MPs) and finer and thinner than those at 1 m (E2), representative of the height of a young child. That is, children might be exposed to more MPs and MRs through inhalation than adults, but these particles are likely to be coarser and less fibrous.

5. Conclusions

In different municipal sectors throughout the city of Shiraz, the accumulation of roadside dusts, MPs and MRs were spatially heterogeneous. However, and regardless of location, all types of solid exhibited a decline in accumulation, and MPs and MRs showed a decrease in concentration (per g of dust), with increasing elevation up to about 1.8 m. Increasing elevation was also associated with a reduction in particle size and percentage of fibres, and in particular for MPs.

The fractionation of MPs and MRs by height is attributed to the resuspension of material by wind and passing traffic and results in exposure scenarios for adults and children in the urban setting that are subtly, but potentially significantly, different.

Acknowledgements

We thank Shiraz University for funding this research.

References

Abbasi, S., Keshavarzi, B., Moore, F., Delshab, H., Soltani, N. & Sorooshian, A. 2017. Investigation of microrubbers, microplastics and heavy metals in street dust: a study in Bushehr city, Iran. Environmental Earth Sciences, 76, 1-19.

Abbasi, S., Keshavarzi, B., Moore, F., Turner, A., Kelly, F. J., Dominguez, A. O. & Jaafarzadeh, N. 2019. Distribution and potential health impacts of microplastics and microrubbers in air and street dusts from Asaluyeh County, Iran. Environmental pollution, 244, 153-164.

Abbasi, S., Rezaei, M., Ahmadi, F. & Turner, A. 2022. Atmospheric transport of microplastics during a dust storm. Chemosphere, 292, 133456.

Adachi, K., Tainosho, Y., 2004. Characterization of heavy metal particles embedded in tire dust. Environment International 30, 1009-1017.

Alvez, C.A., Vicente, E.D., Vicente, A.M.P., Rienda, I.C., Tomé, M., Querol, X., Amato, F., 2020. Science of the Total Environment 737, 139596.

Amato, F., Karanasiou, A., Moreno, T., Alastuey, A., Orza, J.A.G., Lumbreras, J., Borge, R., Boldo, E., Linares, C., Querol, X., 2012. Emission factors from road dust resuspension in a Mediterranean freeway. Atmospheric Environment 61, 580-587.

Amato-Lourenço, L.F., dos Santos Galvão, L., de Wager, L.A., Hiemstra, P.S., Vijver, M.G., Mauad, T., 2020. An emerging class of air pollutants: Potential effects of microplastics to respiratory human health? Science of the Total Environment 749, 141676.

Brahney, J., Hallerud, M., Heim, E., Hahnenberger, M., Sukumaran, S., 2020. Plastic rain in protected areas of the United States. Science 368, 1257-1260.

Cai, K., Li, C., 2019. Street dust heavy metal pollution source apportionment and sustainable management in a typical city - Shijiazhuang, China. Int. J. Res. Public Health 16, 2625.

Dehghani, S., Moore, F., Akhbarizadeh, R., 2017. Microplastic pollution in deposited urban dust, Tehran metropolis, Iran. Environmental Science and Pollution Research. DOI 10.1007/s11356-017-9674-1

Dris R, Gasperi J, Saad M, Mirande C, Tassin B (2016) Synthetic fibers in atmospheric fallout: a source of microplastics in the environment? Mar. Pollut. Bull. 104, 290–293.

Escrig, A., Amato, F., Pandolfi, M., Monfort, E., Querol, X., Celades, I., Sanfélix, V., Alastuey, A., Orza, J.A.G., 2011. Simple estimates of vehicle-induced resuspension rates. Journal of Environmental Management 92, 2855-2859.

Fussell JC, Franklin M, Green DC, Gustafsson M, Harrison RM, Hicks W, Kelly FJ, Kishta F, Miller MR, Mudway IS, Oroumiyeh F, Selley L, Wang M, Zhu Y., 2022. A review of road traffic-derived non-exhaust particles: emissions, physicochemical characteristics, health risks, and mitigation measures. Environ Sci Technol. 56, 6813-6835.

Henn, A.R., 1996. Calculation of the Stokes and Aerodynamic Equivalent Diameters of a Short Reinforcing Fiber. Particle and Particle Systems Characterization 13, 249-253.

Järlskog, I., Strömwvall, A.M., Magnusson, K., Gustafsson, M., Polukarova, M., Galfi, H., Aronsson, M., Andersson-Sköld, Y., 2020. Occurrence of tire and bitumen wear microplastics on urban streets and in sweepsand and washwater. Sci. Total Environ. 729, 138950.

Jung, U., Choi, S.S., 2022. Classification and characterization of tire-road wear particles in road dust by density. Polymers 14, 10.3390/polym14051005

Kitahara, K.I., Nakata, H., 2020. Plastic additives as tracers of microplastic sources in Japanese road dusts. Science of the Total Environment 736, 139694.

Kreider M. L., Panko, J.M., McAtee, B.L., Sweet, L.I., Finley, B.L., 2010. Physical and chemical characterization of tire-related particles: Comparison of particles generated using different methodologies. Science of the Total Environment 408, 652-659.

Kuenen, J.J.P., Visschedijk, A.J.H., Jozwicka, M., Denier van der Gon, H.A.C., 2014. TNO-MACC_II emission inventory; a multi-year (2003e2009) consistent high resolution European emission inventory for air quality modeling. Atmos.Chem. Phys. 14, 10963-10976.

Li, G., Stubblefield, M.A., Garrick, G., Eggers, J., Abadie, C., Huang, B., 2004. Development of waste tire modified concrete. Cement and Concrete Research 34, 2283-2289.

Liu, K., Wu, T., Wang, X., Song, Z., Zong, C., Wei, N., Li, D., 2019. Consistent transport of terrestrial microplastics to the ocean through atmosphere. Environmental Science and Technology 53, 10612-10619.

Mei, D., Wen, M., Xu, X., Zhu, Y., Xing, F., 2018. The influence of wind speed on airflow and fine particle transport within different building layouts of an industrial city. Journal of the Air and Waste Management Association 68, 1038-1050.

Moskovchenko, D.; Pozhitkov, R.; Soromotin, A.; Tyurin, V., 2022. The content and sources of potentially toxic elements in the road dust of Surgut (Russia). Atmosphere 13, 30 https://doi.org/10.3390/atmos13010030

NIVA, 2020. Microplastics in road dust – characteristics, pathways and measures. Report SNO 7526-2020, Norwegian Institute for Water Research (NIVA), Oslo.

O’Brien, S., Okoffo, E.D., Rauert, C., O’Brien, J.W., Ribeiro, F., Burrows, S.D., Toapanta, T., Wang, X., Thomas, K.V., 2021. Quantification of selected microplastics in Australian urban road dust. Journal of Hazardous Materials 416, 125811.

Pandey, D., Banerjee, T., Badola, N., Chauhan, J.S., 2022. Evidences of microplastics in aerosols and street dust: a case study of Varanasi City, India. Environmental Science and Pollution Research https://doi.org/10.1007/s11356-022-21514-1

Panko, J.M., Chu, J., Kreider, M.L., Unice, K.M., 2013. Measurement of airborne concentrations of tire and road wear particles in urban and rural areas of France, Japan, and the United States. Atmospheric Environment 72, 192-199.

Panko, J.M., Hitchcock, K.M., Fuller, G.W., Green, D., 2019. Evaluation of tire wear contribution to PM2.5 in urban environments. Atmosphere 10, 99; doi:10.3390/atmos10020099.

Rienda, I.C., Alves, C.A., 2021. Road dust resuspension: A review. Atmospheric Research 261, 105740.

Rogge, W.F., Hildemann, L.M., Mazurek, M.A., Cass, G.R., 1993. Sources of fine organic aerosol. 3. Road dust, tire debris, and organometallic brake lining dust: Roads as sources and sinks. Environ. Sci. Technol. 27, 1892-1904.

Thatcher, T.L., Layton, D.W., 1995. Deposition, resuspension, and penetration of particles within a residence. Atmospheric Environment 29, 1487-1497.

Thorpe, A., Harrison, R.M., 2008. Sources and properties of non-exhaust particulate matter from road traffic: a review. Sci. Total Environ. 400, 270-282.

Thouron, L., Seigneur, C., Kim, Y., Mahé, F., André, M., Lejri, D., Villegas, D., Bruge, B., Chanut, H., Pellan, Y., 2018. Intercomparison of three modeling approaches for traffic-related road dust resuspension using two experimental data sets. Transportation Research Part D, 58, 108-121.

Venkatram, A., 2000. A critique of empirical emission factor models: a case study of the AP-42 model for estimating PM10 emissions from paved roads. Atmospheric Environment 34, 1-11.

Vethaak, A.D., Legler, J., 2020. Microplastics and human health - knowledge gaps should be addressed to ascertain the health risks of microplastics. Science 371, 672-674.

Wagner, J., Leith, D., 2001. Passive aerosol sampler. Part I: Principle of operation. Aerosol Sci. Technol. 34, 186–192.

Wang, Q., Enyoh, C.E., Chowdury, T., Chowdury, M.A.H., 2020. Analytical techniques, occurrence and health effects of micro and nano plastics deposited in street dust. Int. J. Environ. Anal. Chem. https://doi.org/10.1080/03067319.2020.1811262

Weber, F., Kowarik, I., Säumel, I., 2018. Herbaceous plants as filters: Immobilization of particulates along urban street corridors. Environmental Pollution 186, 234-240.

Weinbruch, S., Worringen, A., Ebert, M., Scheuvens, D., Kandler, K., Pfeffer, U., Bruckmann, P., 2014. A quantitative estimation of the exhaust, abrasion and resuspension components of particulate traffic emissions using electron microscopy. Atmospheric Environment 99, 175-182.

Youn, J.S., Kim, Y.M., Siddiqui, M.Z., Watanabe, A., Han, S., Jeong, S., Jung, Y.W., Jeon, K.J., 2021. Quantification of tire wear particles in road dust from industrial and residential areas in Seoul, Korea.Science of the Total Environment 784, 147177.

Yukioka, S., Tanaka, S., Nabetani, Y., Suzuki, Y., Ushijima, T., Fujii, S., Takada, H., Tran, Q.V., Singh, S., 2020. Occurrence and characteristics of microplastics in surface road dust in Kusatsu (Japan), Da Nang (Vietnam), and Kathmandu (Nepal). Env. Pollut. 256, 113447.

Zhao, H., Jiang, Q., Xie, W., Li, X., Yin, C., 2018. Role of urban surface roughness in road-deposited sediment build-up and wash-off Journal of Hydrology 560, 75-85.